filters," *IEEE Trans. Microwave Theory Tech.*, vol. MTT-19, May 1971.
[8] U. H. Gysel, "New theory and design for hairpin-line filters," *IEEE Trans. Microwave Theory Tech.*, vol. MTT-22, May 1974.
[9] E. G. Cristal, "Microwave filters," in *Modern Filter Theory and Design* G. C. Temes and S. K. Mitra, Eds. New York: Wiley, 1973, pp. 273.
[10] T. A. Milligan, "Dimensions of microstrip coupled-lines and interdigital structures," *IEEE Trans. Microwave Theory Tech.*, vol. MTT-25, May 1977.

Propagation in a Rectangular Waveguide Periodically Loaded with Resonant Irises

MANUEL S. NAVARRO, MEMBER, IEEE, TULLIO E. ROZZI, SENIOR MEMBER, IEEE, AND YUEN TZE LO, FELLOW, IEEE

Abstract—**In this contribution we treat the problem of an infinite rectangular waveguide periodically loaded by means of infinitely thin resonant irises.**

The method of solution breaks down the problem into two separate steps: 1) the multiport network characterization of the resonant iris; 2) the network analysis of the equivalent periodic network.

The results for the resonant iris can be used for various applications, such as the design of waveguide filters and matching networks. In the limiting cases of purely capacitive or inductive irises, the results agree exactly with existing experimental and numerical values.

The size of the eigenvalue equation to be solved for the periodic structure equals half the number of ports of the network characterization of the iris and is generally small (typically five to seven). The eigenvalues have good convergence properties with respect to the size of the matrix.

I. Introduction

In recent years the corrugated waveguide has found wide use in radar and communication systems. Significant research has been done on the problem of the circular corrugated waveguide. We distinguish three main approaches:

1) the modified boundary condition method, applicable only for a special value of the groove depth [1], [2];
2) the modified residue calculus technique [1], [3] applicable only for certain modal configurations;
3) mode matching technique [1] which is fairly general in applicability.

In the case of the rectangular guide, however, method 1) cannot be implemented analytically [3], [4]. Method 2) is altogether not applicable. Method 3) is also not applicable for this kind of geometry owing to the nonseparability of the configuration [4].

Brown in 1958 [5] suggested that a periodically loaded waveguide be modeled by means of a cascade of identical multiport reactances connected by a finite number of uncoupled transmission lines. Each reactance represents a discontinuity in the cascade, which causes coupling between waveguide modes otherwise uncoupled. Unfortunately, up to date this approach could not be actually implemented, due to the lack of proper multiport representation of the discontinuity.

Recently, however, a method for deriving lumped, wide-band equivalent networks of waveguide discontinuities has become available. The above has been applied to the problems of the inductive and capacitive iris and step [6], [7]. Apart from having inherently good convergence properties and involving manipulations with small matrices only, this approach separates the frequency and the geometry dependence, so that the analysis need not be repeated at each frequency point. A detailed discussion has been given elsewhere [6]–[8]. However, for the convenience of the reader, we recall here the concept of "accessible" and "localized" modes. Accessible modes are the waveguide modes that being excited at the location of one discontinuity, are "seen" by the adjacent discontinuities. This includes all the propagating modes of the original (unloaded) waveguide, plus, possibly, the first few evanescent ones, depending upon the separation between adjacent discontinuities.

Each accessible mode corresponds to a pair of accessible ports in the multimode equivalent network of the discontinuity. Between discontinuities, each accessible mode is described by means of a length of transmission line. All remaining modes, purely evanescent, are called localized, as they remain localized to the neighborhood of the discontinuity that excites them. The latter, collectively,

Manuscript received November 14, 1979; revised August 1, 1980.

M. S. Navarro was with the Department of Electrical Engineering, University of Illinois at Urbana, IL. He is now with the Deparmento de Electonica y Circuitos, Universidad Simon Bolivar, Caracas 108, Venezuela.

T. E. Rozzi is with the Department of Electrical Engineering and Electronics, University of Liverpool, Liverpool, L69 3BX U.K.

Y. T. Lo is with the Department of Electrical Engineering, University of Illinois, Urbana, IL.

0018-9480/80/0800-0857$00.75 ©1980 IEEE

gives rise to the energy storage and to the coupling between accessible modes, represented by the reactance of the discontinuity.

The reactance is described by means of its poles and residues, which are functions of the geometry only. Once these data are available for a range of geometries the user need no longer be concerned with the original field problem. The latter has been translated into a standard multiport network analysis problem.

In the case of the periodically loaded rectangular waveguide, the resonant iris is the building block of the structure. Relatively little is known about the resonant iris, apart from early approximate results for the isolated iris [9]. The results we will present here for the resonant iris are also applicable to filter design in waveguides.

The unit cell of the resulting periodic equivalent circuit consists of a lumped multiport reactance enclosed between two sets of parallel transmission lines of equal length. Upon application of the periodicity condition to the unit cell, the problem of determining the propagation constant on the corrugated waveguide reduces to the solution of an eigenvalue equation whose order is equal to the number of accessible modes, typically two to seven. The eigenvalues show good convergence properties as the number of accessible modes is increased.

The transverse fields are described by a linear combination of the accessible modes, with amplitudes determined by the eigenvectors of the eigenvalue equation.

II. The Resonant Iris

The geometry of a single resonant iris is illustrated in Fig. 1. For the purpose of the present application, the iris is supposed to be symmetric and infinitely thin. The analysis can be extended to the case of finite thickness, which might be relevant to other applications, as previously done for the inductive [6] and capacitive [7] iris.

When the iris is excited by the fundamental TE_{10} waveguide mode in a standard waveguide it is a very good approximation to assume that the family of LSE_{x-mn} modes is excited [10], [11]. Owing to the symmetry of the iris, m can only take odd values and n even values.

For propagation in the z direction, the characteristic admittance is defined uniquely as the ratio H_x/E_y, where

$$\phi_i(xy) = E_y = \sqrt{\epsilon_n}\ \sin\frac{m\pi}{a}x\cos\frac{n\pi}{b}y, \qquad i\leftrightarrow(mn),$$

$$\epsilon_n = \begin{cases} \frac{1}{2}, & n=0 \\ 1, & n\neq 0 \end{cases} \tag{1}$$

$$H_x = -Y_{0mn}E_y \tag{2}$$

with

$$Y_{0mn} = \left(\frac{m\pi}{2}\right)^2 - k_0^2 \Big/ j\omega\mu\gamma_{mn} \tag{3}$$

$$\gamma_{mn} = \sqrt{\left(\frac{m\pi}{a}\right)^2 + \left(\frac{n\pi}{b}\right)^2 - k_0^2} \tag{4}$$

We consider k accessible modes at each side of each iris.

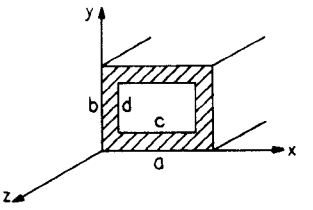

Fig. 1.

Owing to the symmetry and to the fact that the iris is infinitely thin, the resulting $2k$-reactance matrix of the discontinuity is of the form

$$\begin{pmatrix} x & x \\ x & x \end{pmatrix} \tag{5}$$

where x is a $k\times k$ symmetric reactance matrix. The Ritz–Galerkin variational expression for the matrix elements is [6]

$$x_{ij} = \bar{Q}_i^T\cdot(\bar{B})^{-1}\cdot\bar{Q}_j, \qquad 1\leqslant i, \quad j\leqslant k. \tag{6}$$

The N-dimensional vector $\bar{Q}_i$ represents the function $\phi_i(x,y)$ in terms of a complete set of expanding functions satisfying the E_y boundary conditions, $v_\mu(x,y)(1\leqslant\mu\leqslant N)$ truncated after N terms, and is given component wise by

$$\bar{Q}_{\mu i} = \int_0^c\int_0^d \phi_i(x,y)v_\mu(x,y)\,dx\,dy \tag{7a}$$

the components of the $N\times N$ matrix $\bar{B}$ are obtained from the Green's function

$$-j\bar{B}(x,y;x',y') = \sum_{i>k}^{\infty} 2Y_{0i}\phi_i(x,y)\phi_i(x',y') \tag{8}$$

as

$$(\bar{B})_{\mu\nu} = \iiiint_{\text{aperture}} v_\mu(x,y)\bar{B}(x,y;x',y')v_\nu(x',y')\,dx\,dy\,dx'\,dy'. \tag{7b}$$

Observe that, consistently, with their definition, the accessible modes do no appear in the above summation. Only the localized modes contribute to energy storage in the neighborhood of the discontinuity.

In order to improve the convergence of the infinite sum in (8), it is convenient to integrate (7) by parts, making use of the fact that E_y must be zero at the aperture edges: $x=(a\pm c)/2$ [12, p. 349]. Then a more convenient expression for x_{ij} is given by[1]

$$x_{ij} = \boldsymbol{Q}_i^T\cdot\boldsymbol{B}^{-1}\cdot\boldsymbol{Q}_j \tag{9}$$

where $\boldsymbol{Q}_i$ the vector corresponding to the mode potential function

$$\psi_i(x,y) = \frac{\sqrt{\epsilon_n}}{m}\cos\frac{m\pi}{a}\cos\frac{n\pi}{b}y \tag{10}$$

is given by an expression similar to (7a), where ϕ_i is replaced by ψ_i and v_μ by $u_\mu=\partial/\partial_x v_\mu$. $\boldsymbol{B}$ is the matrix associated with

$$-jB(x,y;x',y') = \sum_{ik}^{\infty} 2Y_{0i}\psi_i(x,y)\psi_i(x',y'). \tag{11}$$

[1]The superscript T denotes transposition.

A good choice of a basis for the aperture is provided by the Schwinger's functions, which being derived by conformal mapping of the static fields, inherently satisfy the edge condition for the inductive and capacitive limits. The defining equation is [11, p. 350]

$$\cos\frac{\pi x}{a}=P_{11}\cos\theta \tag{12}$$

where

$$P_{11}=\sin\frac{\pi c}{a} \tag{13}$$

and $\theta=0,\pi$ correspond to $x=(a\mp c)/2$, respectively. The coefficients of the *finite* expansion

$$\cos\frac{m\pi x}{a}=\sum_{p=1,3,\cdots}^{m}P_{mp}\cos p\theta \tag{14}$$

can be found by recursion and are given elsewhere [6], [7]. Similarly, we have

$$\cos\frac{\pi y}{b}=S_{11}\cos\eta \qquad S_{11}=\sin\frac{\pi d}{b} \qquad S_{00}=1$$

$$\eta=\begin{cases}0, & \text{for } y=\dfrac{b-d}{2}\\ \pi & \text{for } y=\dfrac{b+d}{2}\end{cases} \tag{15}$$

$$\cos\frac{n\pi y}{b}=\sum_{q=0,2,\cdots}^{n}S_{nq}\cos q\eta. \tag{16}$$

The required orthonormal basis on the aperture can be built up as

$$\begin{aligned}u_1(\theta,\eta)&=\cos\theta\cdot\frac{1}{\sqrt{2}}\\ u_2(\theta,\eta)&=\cos 3\theta\cdot\frac{1}{\sqrt{2}}\\ u_3(\theta,\eta)&=\cos\theta\cdot\cos 2\eta\\ u_4(\theta,\eta)&=\cos 5\theta\cdot\frac{1}{\sqrt{2}}\\ u_5(\theta,\eta)&=\cos 3\theta\cdot\cos 2\eta\,.\\ &\cdots\qquad\qquad\cdots\end{aligned} \tag{17}$$

The apparently arbitrary ordering will be made clear in the following. Using the basis (17), we can express the modal potentials (10), ordered according to increasing *cutoff* number as follows:

$$\begin{aligned}\psi_{(1,0)}&=P_{11}S_{00}u_1\\ \psi_{(3,0)}&=P_{31}S_{00}u_1+P_{33}S_{00}u_2\\ \psi_{(1,2)}&=P_{11}S_{20}u_1+\quad 0\quad +P_{11}S_{22}u_3\\ \psi_{(5,0)}&=P_{51}S_{00}u_1+P_{53}S_{00}u_2+\quad 0+P_{55}S_{00}u_4\\ &\qquad\cdots\text{etc.}\end{aligned} \tag{18}$$

The waveguide susceptance becomes the matrix

$$-jB_{pq;rs}=\sum_{\substack{m=1,3,5,\cdots,\\ n=0,2,4,\cdots,}}^{\infty'}\frac{2}{m^2}\frac{\epsilon_n}{\sqrt{\epsilon_q}\sqrt{\epsilon_s}}Y_{0mn}P_{mp}S_{nq}P_{mr}S_{ns} \tag{19}$$

where the prime indicates that the accessible modes have been excluded from the summation. Reverting to single index notation, we let l correspond to (m,n), h to (p,q), g to (r,s), so that

$$-jB_{hg}=\sum_{l>k}^{\infty}2Q_{hl}Q_{gl}Y_{0l} \tag{20}$$

where

$$\begin{aligned}Q_{hl}&=\frac{\sqrt{\epsilon_n}}{m\sqrt{\epsilon_q}}P_{mp}S_{nq}\\ Q_{gl}&=\frac{\sqrt{\epsilon_n}}{m\sqrt{\epsilon_s}}P_{mr}S_{ns}.\end{aligned} \tag{21}$$

III. Frequency Dependence and Reactance Matrix

In order to derive a true network model of the discontinuity, we need to consider explicitly the frequency dependence of the reactance. It is expedient to introduce a normalized propagation constant

$$\bar{\beta}=\frac{a}{\pi}\beta_{10}=\sqrt{\left(\frac{2a}{\lambda_0}\right)^2-1} \tag{22}$$

λ_0 being the free-space wavelength. In the following, $\bar{\beta}$ will play the role of an effective frequency variable. The modal characteristic admittances, normalized to that of the fundamental mode, are given by

$$\bar{Y}_{0,mn}(j\bar{\beta})=\frac{m^2-1}{j\bar{\beta}\sqrt{m^2+\left(\frac{a}{b}n\right)^2-1-\bar{\beta}^2}}+\frac{j\bar{\beta}}{\sqrt{m^2+\left(\frac{a}{b}n\right)^2-1-\bar{\beta}^2}}. \tag{23}$$

Observe that for $n=0$, $m>1$, the above reduces to the characteristic admittance of TE_{m0} modes, excited by a purely inductive iris

$$\bar{Y}_{0,m}(j\bar{\beta})=\frac{\sqrt{m^2-\bar{\beta}^2-1}}{j\bar{\beta}}. \tag{24}$$

For localized modes, the above frequency dependence can be approximated over a broad band by means of a positive real lumped admittance corresponding to a parallel *LC*

$$Y_{0,m}(\bar{\beta})=k_1^{(m)}\frac{\sqrt{m^2-1}}{j\bar{\beta}}+\frac{k_2^{(m)}}{2}\frac{j\bar{\beta}}{\sqrt{m^2-1}}. \tag{25}$$

The positive constant $k_1^{(m)}$, $k_2^{(m)}$ are close to unity and tend to 1 as $m\to\infty$. Given a band of interest, they are determined for each m by minimizing the maximum absolute deviation of

$$|\bar{Y}_{0,m}(j\bar{\beta})-Y_{0,m}(j\bar{\beta})|$$

in the Chebyshev sense over the band. The high degree of accuracy of this approximation has been demonstrated previously [6]. When $m=1$, $n>0$ the modal admittance reduces to

$$\bar{Y}_{0,1n}(j\bar{\beta})=\frac{b}{a}\frac{j\bar{\beta}}{\sqrt{n^2-\left(\frac{b}{a}\bar{\beta}\right)^2}} \tag{26}$$

which is the admittance of the LSE_{1n} modes excited by a purely capacitive iris. The above expression can be approximated by a pure capacitance in $\bar{\beta}$

$$y_{0,1n}(j\bar{\beta})=k_3^{(n)}\frac{b}{na}j\bar{\beta}. \tag{27}$$

The positive constant $k_3^{(n)}$ is close to unity and$\rightarrow 1$ as $n\rightarrow\infty$. For each n, it is determined by minimizing the maximum value of

$$|\bar{Y}_{0,1n}(j\bar{\beta})-y_{0,1n}(j\bar{\beta})|$$

in the Chebyshev sense over the band of interest. As an example of the accuracy of this approximation, for the worst case: $n=2$, corresponding to one accessible mode, for $b/a=4/9$ (standard waveguide), in the band $0.3\leqslant\bar{\beta}\leqslant 1.6$, we obtain a maximum error of 1.6 percent. The error reduces to 0.6 percent for $k_3^{(2)}=1.0124$ in the range to $1.0\leqslant\bar{\beta}\leqslant 1.6$, which is the standard waveguide band.

As the error decreases drastically with increasing n (about a factor 10 for each successive value of n) the frequency band can be extended at will by considering more modes to be accessible. In the general case, $m>1$, $n>0$, the admittance (23) can be approximated by another parallel LC in $\bar{\beta}$

$$Y_{0,i}(j\bar{\beta})=\frac{k_4^{(i)}}{j\bar{\beta}}\frac{m^2-1}{c_i}+\frac{k_5^{(i)}j\bar{\beta}}{c_i} \tag{28}$$

where $i\leftrightarrow(m,n)$, $c_i=\sqrt{m^2-(a/bn)^2-1}$, and $k_4^{(i)}$ and $k_5^{(i)}$ are positive constants close to unity with $k_4^{(i)}\rightarrow 1$ as either m or $n\rightarrow\infty$. For a given n, $k_5^{(i)}\rightarrow 1$ as $m\rightarrow\infty$. These constants can be determined with the same procedure as above.

The error incurred in (28) is only a small fraction of that involved in the approximation in (27). In fact, (27) sets the overall limit to the accuracy of the lumped approximation. Introducing now the lumped frequency approximation (25), (27), and (28) in the expression (20) for the susceptance matrix, we obtain

$$\boldsymbol{B}(\bar{\beta})=\frac{1}{\bar{\beta}}(\boldsymbol{L}^{-1}-\bar{\beta}^2\boldsymbol{C}) \tag{29}$$

where we introduce the constant, positive definite matrices

$$\boldsymbol{L}^{-1}=(\boldsymbol{L}^{\text{ind}})^{-1}+(\boldsymbol{L}^{\text{res}})^{-1} \tag{30}$$

$$\boldsymbol{C}=\boldsymbol{C}^{\text{ind}}+\boldsymbol{C}^{\text{cap}}+\boldsymbol{C}^{\text{res}} \tag{31}$$

with

$$(L^{\text{ind}})_{hg}^{-1}=\sum_{m=1}k_1^{(m)}\sqrt{\frac{m^2-1}{m^2}}\,P_{mp}P_{mr} \tag{32}$$

$h\leftrightarrow(p,0)$, $g\leftrightarrow(r,0)$, and the indexing follows the scheme given in (17). Also,

$$(L^{\text{res}})_{hg}^{-1}=\sum_{\substack{m=1,3\cdots\\ n=0,2\cdots}}k_4^{(m,n)}\frac{\epsilon_n}{\sqrt{\epsilon_s\epsilon_q}}\frac{1}{c_i}\frac{1}{m^2}P_{mp}S_{nq}P_{mr}S_{ns},$$

$$h=(p,q),\qquad g\leftrightarrow(r,s) \tag{33}$$

$$C_{hg}^{\text{ind}}=\sum_{m=1,2}\frac{k_2^{(m)}}{\sqrt{m^2-1}}\frac{1}{m^2}P_{mp}P_{mr} \tag{34}$$

h and g are the same as in connection with (32)

$$C_{hg}^{\text{cap}}=\sum_{\substack{m=1\\ n=0,2\cdots}}{}'\frac{k_3^{(n)}}{\left(\frac{a}{b}n\right)}\frac{\epsilon_n}{\sqrt{\epsilon_q\epsilon_s}}P_{11}^2S_{nq}S_{ns} \tag{35}$$

$$C_{hg}^{\text{res}}=\sum_{\substack{m=1,3\cdots\\ n=2,4\cdots}}{}'\frac{k_5^{(m,n)}}{c_i}\frac{1}{m^2}\frac{n}{\sqrt{\epsilon_s\epsilon_q}}P_{mp}S_{nq}P_{mr}S_{ns}. \tag{36}$$

We recognize that $(\boldsymbol{L}^{\text{ind}})^{-1}$ corresponds to the inductive contribution (magnetic storage) of an inductive iris having width identical to that of the resonant iris. $\boldsymbol{C}^{\text{ind}}$ is the capacitive contribution associated with the above inductive iris (electric storage). $\boldsymbol{C}^{\text{cap}}$ is the capacitive contribution of a capacitive iris having the same height as the resonant iris. $\boldsymbol{L}^{\text{res}}$ and $\boldsymbol{C}^{\text{res}}$ are the inductive and capacitive contributions, respectively, particular to the resonant character of the iris.

As $\boldsymbol{L}$ and $\boldsymbol{C}$ are positive definite, constant symmetric matrices, they can be diagonalized and $\boldsymbol{B}$ can be formally inverted. As a result we have

$$\boldsymbol{B}^{-1}(\bar{\beta})=\bar{\beta}\boldsymbol{M}^T(\boldsymbol{I}-\bar{\beta}^2\Lambda)^{-1}\boldsymbol{M} \tag{37}$$

where

$$\boldsymbol{M}=\boldsymbol{T}^T\boldsymbol{L}^{1/2}$$
$$\boldsymbol{L}^{1/2}\boldsymbol{C}\boldsymbol{L}^{1/2}=\boldsymbol{T}\Lambda\boldsymbol{T}^T \tag{38}$$

and Λ is the diagonal matrix of the eigenvalues of (38).

Introducing now (37) into (9) we obtain

$$x_{ij}(\bar{\beta})=\bar{\beta}\sum_{v=1}^{N}\frac{(\boldsymbol{M}\cdot\boldsymbol{Q}_i)_v^T(\boldsymbol{M}\cdot\boldsymbol{Q}_j)_v}{1-\left(\frac{\bar{\beta}}{\bar{\beta}_v}\right)^2} \tag{39}$$

$$=\sum_{v=1}^{N}\frac{r_{ij}^{(v)}\bar{\beta}}{1-\left(\frac{\bar{\beta}}{\bar{\beta}_v}\right)^2},\qquad 1\leqslant i,\quad j\leqslant k \tag{40}$$

where $1/\bar{\beta}_v^2$ is the vth element of the positive definite diagonal matrix Λ, N is the order of the matrix $\boldsymbol{B}$, i.e., the order of the variational solution. We recognize in (40) the Foster canonical form of the reactance. The poles $\bar{\beta}_v$ and the corresponding residue matrices are functions of the

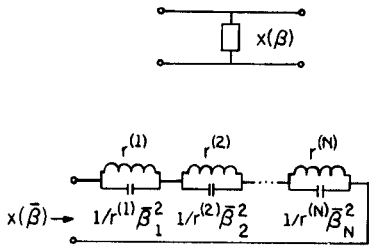

Fig. 2.

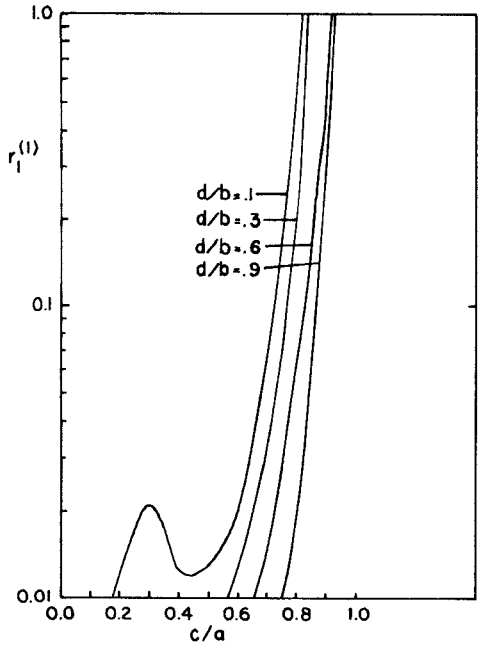

Fig. 3. Residue ($v=1$), resonant iris.

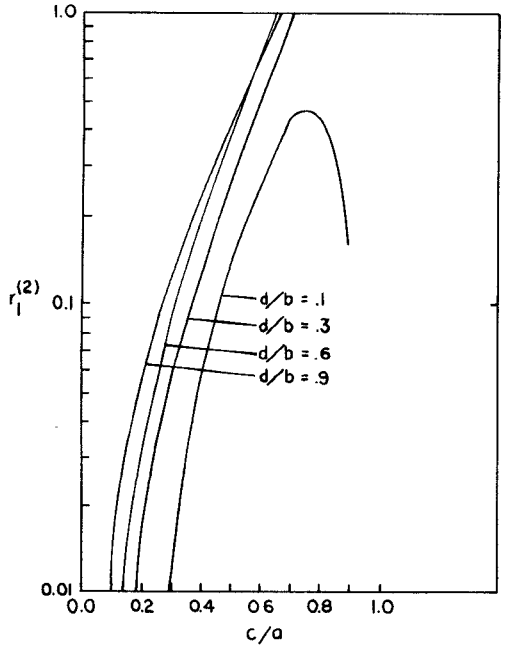

Fig. 4. Residue ($v=1$), resonant iris.

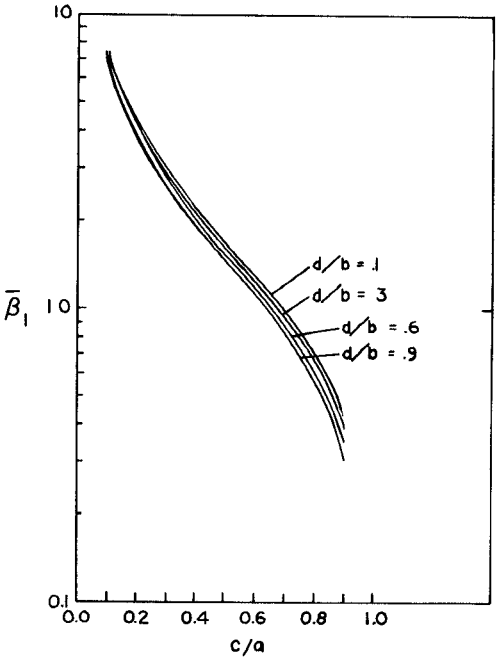

Fig. 5. Residue ($v=1$), resonant iris.

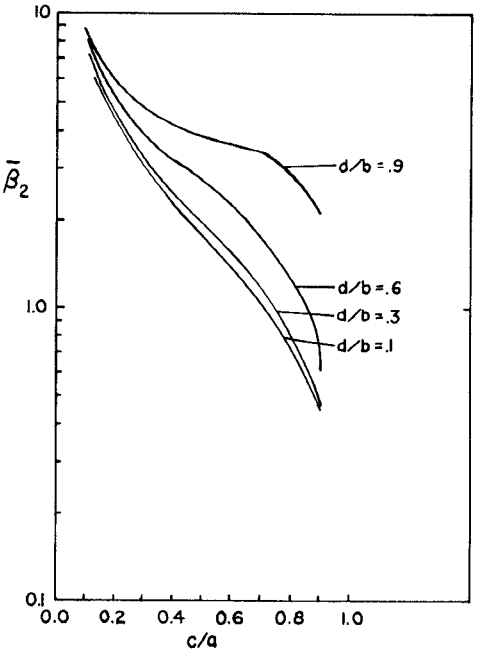

Fig. 6. Pole ($v=2$), resonant iris.

geometry only and they satisfy the convergence requirements described in [8].

A frequency independent lumped network model of the iris can be derived from (40). For one accessible mode, this is illustrated in Fig. 2. Poles and residues for one accessible mode are plotted in Figs. 3–6 over a wide range of aperture dimensions for a waveguide of standard aspect ratio ($a/b=9/4$). The constants k_1-k_5 were computed for the frequency range $1 \leqslant \bar{\beta} \leqslant 1.6$, corresponding to the standard wave guide band. However, the resulting model remains accurate even for frequencies somewhat beyond the band.

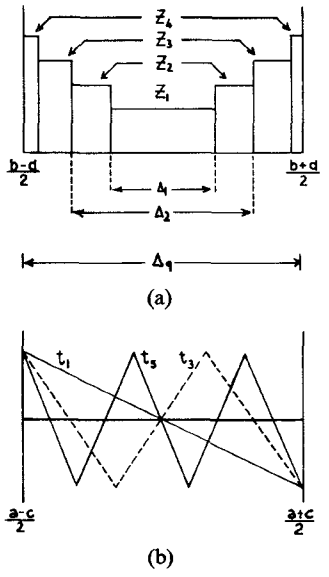

Fig. 7. (a) y-dependent basis functions. (b) x-dependent basis functions.

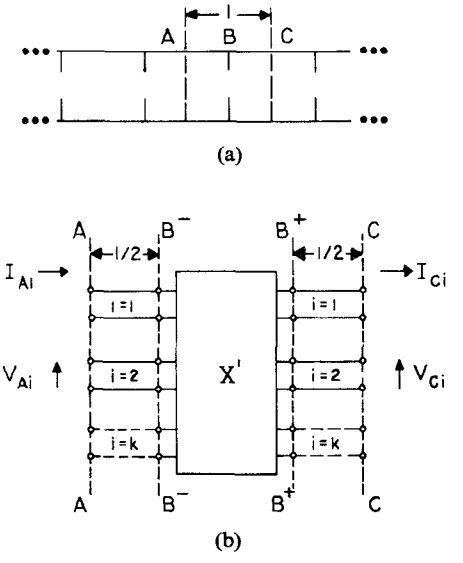

Fig. 8. (a) Side view of corrugated guide. (b) Network model of unit cell.

As a check, the cases of the inductive and capacitive iris can be recovered by letting $d/b \to 1$ and $c/a \to 1$, respectively. The numerical results agree closely with those previously obtained in [6] and [7], respectively. Poles and residues for two and three accessible modes have also been computed and can be found in [4]. The above results eliminate the need of a field analysis program studying a cascade of interacting resonant irises, such as in filters and corrugated structures. The latter application will be further pursued in the following.

IV. An Alternative Expanding Set

The choice of Schwinger's functions as a basis is particularly convenient when the resonants iris approaches either the capacitive ($c/a \to 1$) or the inductive limit ($d/b \to 1$), as then the quasi-static contribution can be extracted and summed analytically.

For the general case, however, most of the computational effort is involved in summing the series for the "resonant" terms, i.e., $M > 1$, $N > 0$.

With a view to summing those terms efficiently, we have examined another choice of expanding set. This consists in taking pulse functions in the y direction and linear odd functions in the x direction, as shown in Fig. 7(a) and (b). The functions of the above set are obviously independent and take account of the symmetry of the field as well as of the boundary conditions.

A discussion of this question is omitted here for the sake of brevity, but the details can be found in [4].

V. Corrugated Rectangular Waveguide

A side view of the geometry is given in Fig. 8(a). The unit cell of the periodic structure is defined as shown between reference planes AA and CC. The equivalent network of the unit cell is illustrated in Fig. 8(b). This consists of the lumped reactance

$$\boldsymbol{X}' = \left(\begin{array}{c|c} \overset{k}{\boldsymbol{x}} & \overset{k}{\boldsymbol{x}} \\ \hline \boldsymbol{x} & \boldsymbol{x} \end{array}\right) \begin{matrix} k \\ k \end{matrix} \tag{41}$$

where $\boldsymbol{x}$ is given by (40) and k is the number of accessible modes.

The lumped reactance is enclosed between two sets of k parallel uncoupled transmission lines of length $l/2$, l being the length of the unit cell.

The transfer ($ABCD$) matrix of the reactance is

$$\begin{pmatrix} \boldsymbol{V} \\ \boldsymbol{I} \end{pmatrix}_{B-} = \left(\begin{array}{c|c} \boldsymbol{U} & 0 \\ \hline -j\boldsymbol{x}^{-1} & \boldsymbol{U} \end{array}\right) \begin{pmatrix} \boldsymbol{V} \\ \boldsymbol{V} \end{pmatrix}_{B+} \tag{42}$$

where $\boldsymbol{U}$ is the unit matrix of order k. The transfer matrix for the length $l/2$ of the multiple transmission line is

$$\begin{pmatrix} \boldsymbol{V} \\ \boldsymbol{I} \end{pmatrix}_{A} = \begin{pmatrix} \boldsymbol{Ch} & \boldsymbol{Z \cdot Sh} \\ \boldsymbol{Z}^{-1}\boldsymbol{Sh} & \boldsymbol{Ch} \end{pmatrix} \begin{pmatrix} \boldsymbol{V} \\ \boldsymbol{I} \end{pmatrix}_{B-} \tag{43}$$

where

$$\boldsymbol{Ch} = \operatorname{diag}(\cosh \gamma_1 l/2, \cosh \gamma_2 l/2, \cdots, \cosh \gamma_k l/2)$$

$$\boldsymbol{Sh} = \operatorname{diag}(\sinh \gamma_1 l/2, \sinh \gamma_2 l/2, \cdots, \cosh \gamma_k l/2)$$

$$\boldsymbol{Z} = \operatorname{diag}\left(1, \bar{Y}_{02}^{-1}, \cdots, \bar{Y}_{0k}^{-1}\right). \tag{44}$$

The total transfer matrix between reference planes $A-A$ and $C-C$ is the product of the three individual transfer matrices, i.e.,

$$\boldsymbol{R} = \begin{pmatrix} \boldsymbol{T} & \boldsymbol{W} \\ \boldsymbol{V} & \boldsymbol{T}^{T} \end{pmatrix} = \begin{pmatrix} \boldsymbol{Ch} & \boldsymbol{ZSh} \\ \boldsymbol{Z}^{-1}\boldsymbol{Sh} & \boldsymbol{Ch} \end{pmatrix} \begin{pmatrix} \boldsymbol{U} & 0 \\ -j\boldsymbol{x}^{-1} & \boldsymbol{U} \end{pmatrix} \cdot \begin{pmatrix} \boldsymbol{Ch} & \boldsymbol{ZSh} \\ \boldsymbol{Z}^{-1}\boldsymbol{Sh} & \boldsymbol{Ch} \end{pmatrix}. \tag{45}$$

The two submatrices on the main diagonal of $\boldsymbol{R}$ are transposed of each other, owing to the longitudinal sym-

metry of the network. The matrix $\boldsymbol{T}$ is given by

$$\boldsymbol{T}=\operatorname{diag}(\cosh\gamma_i l)-j\boldsymbol{Z}\cdot\boldsymbol{Sh}\cdot\boldsymbol{x}^{-1}\cdot\boldsymbol{Ch}. \tag{46}$$

This is in fact the only matrix which will be needed in the following. Imposing the condition that the structure satisfy Floquet's theorem implies that

$$\begin{pmatrix}\boldsymbol{V}\\ \boldsymbol{I}\end{pmatrix}_A=e^{\theta l}\begin{pmatrix}\boldsymbol{V}\\ \boldsymbol{I}\end{pmatrix}_C \tag{47}$$

but, since

$$\begin{pmatrix}\boldsymbol{V}\\ \boldsymbol{I}\end{pmatrix}_A=\boldsymbol{R}\cdot\begin{pmatrix}\boldsymbol{V}\\ \boldsymbol{I}\end{pmatrix}_C. \tag{48}$$

The transfer matrix of the unit cell must satisfy the eigenvalue equation

$$\boldsymbol{R}\begin{pmatrix}\boldsymbol{V}\\ \boldsymbol{I}\end{pmatrix}=e^{\theta l}\begin{pmatrix}\boldsymbol{V}\\ \boldsymbol{I}\end{pmatrix} \tag{49}$$

where θ is the propagation constant of the structure, the vector $(\boldsymbol{V},\boldsymbol{I})^{\mathrm{T}}$ determines the y-directed electric and x-directed magnetic fields of the eigenmodes of the structure, i.e.,

$$\begin{aligned}E_y(x,y)&=\sum_{i=1}^{k}V_i\phi_i(x,y)\\ -H_x(x,y)&=\sum_{i=1}^{k}I_i\phi_i(x,y).\end{aligned} \tag{50}$$

The remaining field components can be derived through Maxwell's equations. The solution of the eigenvalue equation (49) is simplified if we consider the following analytical properties of the matrix $\boldsymbol{R}$.

We observe first of all that if (49) is satisfied, then the following eigenvalue equation is also satisfied.

$$\tfrac{1}{2}(\boldsymbol{R}+\boldsymbol{R}^{-1})\begin{pmatrix}\boldsymbol{V}\\ \boldsymbol{I}\end{pmatrix}=\tfrac{1}{2}(e^{\theta l}+e^{-\theta l})\begin{pmatrix}\boldsymbol{V}\\ \boldsymbol{I}\end{pmatrix}=\cosh\theta l\begin{pmatrix}\boldsymbol{V}\\ \boldsymbol{I}\end{pmatrix}. \tag{51}$$

The above equation proves the physically intuitive fact that if θ is a propagation constant of the structure, then $-\theta$ is also a propagation constant.

Inspection of (45) shows that $\boldsymbol{R}^{-1}$ is obtained by replacing $\boldsymbol{Sh}$ by $-\boldsymbol{Sh}$ and $\boldsymbol{x}$ by $-\boldsymbol{x}$. As a consequence, we have

$$\boldsymbol{R}^{-1}=\begin{pmatrix}\boldsymbol{T} & -\boldsymbol{W}\\ -\boldsymbol{V} & \boldsymbol{T}^{T}\end{pmatrix} \tag{52}$$

so that

$$\tfrac{1}{2}(\boldsymbol{R}+\boldsymbol{R}^{-1})=\begin{pmatrix}\boldsymbol{T} & 0\\ 0 & \boldsymbol{T}^{T}\end{pmatrix}. \tag{53}$$

Some $\boldsymbol{T}$ and $\boldsymbol{T}^{T}$ have the same eigenvalues, it is sufficient to consider the reduced eigenvalue equation

$$\boldsymbol{T}\cdot\boldsymbol{V}=\cosh\theta l\boldsymbol{V}. \tag{54}$$

The matrix $\boldsymbol{T}$ is real, but not symmetric and therefore, its eigenvalues are complex in general. Only for certain ranges of frequency and combinations of geometry θ will become imaginary, describing a propagating mode. Equation (54) is difficult to solve analytically and must be solved numerically.

TABLE I
CAPACITIVELY LOADED WAVEGUIDE $\bar{\theta}=\theta a$, $l/a=1/16$

	β							
	1.0	1.1	1.2	1.3	1.4	1.5	1.6	k
$\bar{\theta}_1$	j4.416	j4.859	j5.301	j5.744	j6.188	j6.631	j7.075	1
$\bar{\theta}_2$	-	-	-	-	-	-	-	
$\bar{\theta}_1$	j3.937	j4.334	j4.732	j5.131	j5.531	j5.933	j6.336	3
$\bar{\theta}_2$	11.276	11.112	10.93	10.729	10.506	10.262	9.994	
$\bar{\theta}_1$	j3.936	j4.333	j4.731	j5.13	j5.53	j5.932	j6.335	5
$\bar{\theta}_2$	9.757	9.713	9.647	9.558	9.445	9.307	9.143	
$\bar{\theta}_1$	j3.937	j4.334	j4.732	j5.131	j5.531	j5.933	j6.336	7
$\bar{\theta}_2$	14.385	14.177	13.945	13.688	13.404	13.091	12.748	

TABLE II
CAPACITIVELY LOADED WAVEGUIDE $\bar{\theta}=\theta a$, $l/a=1/32$

	β							
	1.0	1.1	1.2	1.3	1.4	1.5	1.6	k
$\bar{\theta}_1$	j5.395	j5.935	j6.476	j7.016	j7.557	j8.099	j8.64	1
$\bar{\theta}_2$	-	-	-	-	-	-	-	
$\bar{\theta}_1$	j4.452	j4.903	j5.354	j5.808	j6.263	j6.72	j7.18	3
$\bar{\theta}_2$	13.648	13.452	13.234	12.992	12.726	12.434	12.114	
$\bar{\theta}_1$	j4.45	j4.901	j5.353	j5.806	j6.261	j6.719	j7.178	5
$\bar{\theta}_2$	9.951	9.924	9.875	9.802	9.706	9.585	9.436	
$\bar{\theta}_1$	j4.53	j4.903	j5.355	j5.808	j6.263	j6.72	j7.179	7
$\bar{\theta}_2$	18.726	18.453	18.15	17.813	17.441	17.033	16.585	

VI. EXAMPLES ON NUMERICAL RESULTS

In the following examples a seventh-order variational solution was used, i.e., the dimension of the matrix B in (9) was seven by seven. Owing to the variational character of the approach and to the choice of basis functions the above number turned out to be sufficient to assure good accuracy of the field representation by any choice of the iris dimensions.

A. Capacitively Loaded Waveguide

As a first example, let us consider a waveguide periodically loaded with capacitive irises.

The solution for this case can be recovered from the general solution by setting $c/a=1$, $m=1$ in Section III, corresponding to the excitation of LSE_{ln} modes. Hence $\boldsymbol{L}^{-1}=0$ and $\boldsymbol{C}=\boldsymbol{C}^{\mathrm{cap}}$ in (29).

Tables I and II display the lowest two eigenvalues of the periodic structure versus the effective frequency $\bar{\beta}$ in the band $1\leqslant\bar{\beta}\leqslant 1.6$ for 1, 3, 5, and 7 accessible modes for the following dimensions: $b/a=4/9$, $d/b=0.6$. For these iris dimensions, the excitation of higher order modes is

TABLE III
INDUCTIVELY LOADED WAVEGUIDE $\bar{\theta}=\theta a$, $l/a=1/16$

	β							
	1.0	1.1	1.2	1.3	1.4	1.5	1.6	k
$\bar{\theta}_1$	-	-	-	-	-	-	-	1
$\bar{\theta}_2$	6.387	6.172	5.925	5.644	5.324	4.957	4.532	
$\bar{\theta}_1$	j22.879	j18.731	j15.292	j.0.675	j1.775	j2.460	j2.076	3
$\bar{\theta}_2$	2.535	2.082	1.428	31.197	31.09	30.975	30.852	
$\bar{\theta}_1$	j32.597	j21.758	j14.865	j9.461	j3.704	j1.517	j2.325	5
$\bar{\theta}_2$	3.018	2.652	2.179	1.502	0.593	j1.791	j2.514	
$\bar{\theta}_1$	C	C	C	j17.034	j1.247	j2.078	j2.706	7
$\bar{\theta}_2$	2.697	2.323	1.816	0.992	j0.974	j1.915	j2.521	

TABLE V
WAVEGUIDE LOADED WITH RESONANT IRISES $\bar{\theta}=\theta a$, $l/a=1/8$

	β							
	1.0	1.1	1.2	1.3	1.4	1.5	1.6	k
$\bar{\theta}_1$	j2.924	j3.340	j3.744	j4.138	j4.526	j4.910	j5.290	1
$\bar{\theta}_2$	-	-	-	-	-	-	-	
$\bar{\theta}_1$	j2.695	j3.129	j3.530	j3.934	j4.319	j4.698	j5.072	3
$\bar{\theta}_2$	10.877	10.757	10.625	10.48	10.323	10.151	9.964	
$\bar{\theta}_1$	j2.470	j2.903	j3.314	j3.712	j4.099	j4.482	j4.859	5
$\bar{\theta}_2$	11.393	11.379	11.354	11.315	11.263	11.197	11.116	
$\bar{\theta}_1$	j2.643	j3.062	j3.459	j3.845	j4.223	j4.596	j4.966	7
$\bar{\theta}_2$	12.092	11.985	11.887	11.782	11.666	11.539	11.399	

considerable and therefore we expect, in principle, strong interaction between closely spaced irises.

The spacing l/a equals 1/16 in Table I and 1/32 in Table II.

In fact, even for this close spacing, three accessible modes seem to be sufficient to describe accurately the effect of interaction.

B. Inductively Loaded Waveguide

The case of the inductively loaded waveguide can be recovered from the general theory by setting $d/b=1$ and $n=0$ in Section III, corresponding to the excitation of TE_{m0} modes. Hence, $\boldsymbol{L}=\boldsymbol{L}^{\text{ind}}$ in (37) and $\boldsymbol{C}=\boldsymbol{C}^{\text{ind}}$ in (38). Table III shows the eigenvalues for 1, 3, 5, and 7 accessible modes over the band $1\leqslant\bar{\beta}\leqslant 1.6$ for the waveguide dimensions $b/a=4/9$, $c/a=0.6$ and for the spacing $l/a=1/16$.

The slower convergence of the eigenvalues with increasing number of accessible modes, as compared to the capacitive case, is a consequence of the fact that the cutoff numbers of higher order TE_{m0} modes increase more slowly than those of LSE_{1n} modes.

C. Waveguide Loaded with Resonant Irises

In the general case when c/a and d/b are less than unity, the whole family of LSE_{mn} modes is excited. Considering the cutoff characteristics of these modes, we expect even stronger interaction and, consequently, slower convergence of the eigenvalues with increasing number of accessible modes.

In the example illustrated in Tables IV and V, the iris dimensions were $c/a=0.8$, $d/b=0.6$ and the spacings were chosen to $l/a=1/4$ and 1/8, respectively. The latter spacing being close to the required value for practical applications.

About seven accessible modes were required in order to ensure convergence of the eigenvalues in the above examples.

Some comments are in order with respect to the number and the ordering of the accessible modes in modelling the resonant iris.

TABLE IV
WAVEGUIDE LOADED WITH RESONANT IRISES $\bar{\theta}=\theta a$, $l/a=1/4$

	β							
	1.0	1.1	1.2	1.3	1.4	1.5	1.6	k
$\bar{\theta}_1$	j2.687	j3.22	j3.718	j4.192	j4.65	j5.098	j5.536	1
$\bar{\theta}_2$	-	-	-	-	-	-	-	
$\bar{\theta}_1$	j2.382	j2.934	j3.426	j3.887	j4.329	j4.757	j5.176	3
$\bar{\theta}_2$	13.323	13.191	13.056	12.911	12.754	12.586	12.403	
$\bar{\theta}_1$	j2.147	j2.694	j3.185	j3.645	j4.087	j4.516	j4.936	5
$\bar{\theta}_2$	12.83	12.767	12.716	12.661	12.597	12.523	12.437	
$\bar{\theta}_1$	j2.395	j2.903	j3.368	j3.808	j4.234	j4.651	j5.06	7
$\bar{\theta}_2$	15.188	14.732	14.525	14.356	14.191	14.02	13.84	

In principle, the ordering of the accessible modes is quite arbitrary. Here we have chosen the criterion of increasing cutoff. According to the geometry, however, the excitation of some modes with higher cutoff number, may be more significant than that of modes with lower cutoff number. The off-diagonal elements of the reactance matrix give the measure of this excitation.

The amplitude of the reactance matrix element times the exponential decay factor:

$$|x_{1n}|^{e^{-\gamma_{n}l}}$$

is, in fact, a good measure of the relative importance of the mode "n". Hence, the ordering chosen here is not necessarily the optimum when working with irises of fixed geometry, in the sense that a different ordering could then be found which minimizes the number of accessible modes needed in the model. This is an important consideration with regard to modeling. Another comment is in order with regard to the singularities of the reactance. Since we have neglected losses, the reactance poles occur at real frequencies and it is possible for some of the poles to lie in the frequency band. These singularities are im-

portant in determining the frequency behavior of the eigenvalues of the periodic structure.

VII. Conclusions

We have presented wide-band equivalent circuits of closely resonant irises in rectangular waveguides. Poles and residues as functions of the geometry are provided so that the user need not refer to a computer program.

The above equivalent circuits constitute the building blocks of the network representation of an infinite waveguide periodically loaded with resonant irises, which we have investigated. The particular cases of capacitively and inductively periodically loaded waveguides are recovered from the general solution. The same network approach can be applied to waveguides loaded with other discontinuities.

References

[1] M. J. Al-Hakkak and Y. T. Lo, "Circular waveguides and horns with anisotropic and corrugated boundaries," Department of Electrical Engineering, Engineering Experiment Station, University of Illinois, Urbana, IL, Antenna Lab. Rep. No. 73-3, 1973.
[2] Y. T. Lo, "Feed investigation for large Thomson scatter radar," Dep. Elec. Eng., Univ. of Illinois, Urbana, IL, Aero. Rep. No. 23, Oct. 1967.
[3] R. Mittra and S. Lee, *Analytical Techniques in the Theory of Guided Waves*. New York, MacMillan, 1974.
[4] M. Navarro, "On waveguides with anisotropic and corrugated boundaries," Ph.D. dissertation, Elec. Eng. Dep. Univ. Illinois, Urbana, IL, 1976.
[5] J. Brown, "Propagation in coupled transmission line systems," *Quant. J. Mech. Appl. Math.*, vol. XI, pt. 2, pp. 235–243, 1958.
[6] T. E. Rozzi and W. F. G. Mecklenbrauker, "Wide-band network modeling of interacting inductive irises and steps," *IEEE Trans. Microwave Theory Tech.*, vol. MTT-23, pp. 235–245, Feb. 1975.
[7] T. E. Rozzi, "A new approach to the network modeling of capacitive irises and steps in waveguide," *Int. J. Circuit Theory Appl.*, vol. 3, pp. 339–354, Dec. 1975.
[8] T. Rozzi, "Network analysis of strongly coupled transverse apertures in waveguides," *Int. J. Circuit Theory Appl.*, vol. 1, pp. 161–178, June 1973.
[9] L. Lewin, *Advanced Theory of Waveguides*. London:Illiffe; 1952, p. 88.
[10] R. J. Mailloux: "Radiation and near field coupling between two co-linear open-ended waveguides," *IEEE Trans. Antennas Propagat.*, vol. AP-17, pp. 49–54, Jan. 1969.
[11] A. Jamieson and T. Rozzi, "Rigorous analysis of cross-polarization in flange-mounted rectangular waveguide radiators," Electron. Lett., vol. 13, no. 24, pp. 742–744, Nov. 1977.
[12] R. Collin, *Field Theory of Guided Waves*. New York:McGraw-Hill, 1962, p. 348.

Transmission Characteristics and a Design Method of Transmission-Line Low-Pass Filters with Multiple Pairs of Coincident Zeros and Multiple Pairs of Coincident Poles

JUNZI HURUYA AND RISABURO SATO, FELLOW, IEEE

Abstract—**The transmission characteristics and a design method are presented for a transmission-line low-pass filter with multiple pairs of coincident zeros in the finite frequency of the passband and multiple pairs of coincident poles in the finite frequency of the stopband and for a transmission-line low-pass filter with Butterworth characteristic in the passband and multiple pairs of coincident poles in the finite frequency of the stopband. The former transmission-line low-pass filter shows an improved skirt attenuation performance and delay characteristic than a Chebyshev transmission-line low-pass filter in the same network degree. The latter type of transmission-line low-pass filter shows an improved skirt attenuation performance in comparison to a Butterworth transmission-line low-pass filter in the same network degree, it is positioned about in the middle between a Butterworth type and a Chebyshev type, the delay characteristic is improved considerably in comparison to the Chebyshev type, and the characteristic is close to that of the Butterworth type.**

With this design method, the connecting unit elements in addition to the stubs contribute to the attenuation response. The design example is shown on the basis of a concrete specification, and it is shown that the obtained attenuation strictly fulfills the specification.

Manuscript received December 10, 1979; revised April 1, 1980.

J. Huruya is with the Department of Education, Yamaguchi University, Yamaguchi, Japan 753.

R. Sato is with the Department of Information Sciences, Tohoku University, Sendai, Japan 980.

I. Introduction

RECENTLY, Levy [1] has shown a lumped element rational function having single transmission zeros in one point of the stopband of a Chebyshev low-pass filter which shows improvement of the skirt selectivity over an ordinary Chebyshev low-pass filter. By use of cross coupling, the realization of a high frequency filter is executed. Further, M. C. Agarwal [2] has proposed a lumped element rational function having multiple pairs of coincident

0018-9480/80/0800-0865$00.75 ©1980 IEEE